SEMARAK ILMU PUBLISHING

Semarak Engineering Journal

Journal homepage:
https://semarakilmu.my/index.php/sej/index
ISSN: 3036-0145



Valorizing Coal Fly Ash in Graphene-Reinforced Aluminum Hybrid Composites: Taguchi Optimization of Powder Metallurgy Parameters

Qomarul Hadi[1], Irsyadi Yani[2,*], Nukman[2], Agung Mataram[2]

[1] Doctoral Program in Engineering Science, Faculty of Engineering, Universitas Sriwijaya, Palembang, Sumatera Selatan, Indonesia
[2] Department of Mechanical Engineering, Faculty of Engineering, Universitas Sriwijaya, Indralaya 30662, South Sumatra, Indonesia

ARTICLE INFO

Article history:
Received 12 August 2026
Received in revised form 13 October 2026
Accepted 21 October 2026
Available online 30 October 2026

Keywords:
Aluminum matrix composite; fly ash valorization; graphene nanoplatelets; powder metallurgy; Taguchi optimization.

ABSTRACT

This study screens four powder-metallurgy variables for reported aluminum/carbon-reinforcement/fly-ash composites (5–15 wt% total reinforcement) using a Taguchi L9 array. Hardness (three indents per condition) varied from 48.13 to 50.07 VHN; Archimedes bulk density varied from 2.493 to 2.560 g/cm³. Main-effect allocations ranked milling time (56.55%) and reinforcement fraction (32.56%) highest for hardness, but holding time (38.24%) and sintering temperature (32.62%) highest for density. These are descriptive screening contributions because the L9 design is saturated. The hardness model predicts approximately 50.37 VHN at 15 wt% reinforcement, 2 h milling, 550 °C and 0.5 h holding. A reported ≈4.4% confirmation gain lacks raw replicate data and uncertainty; its implied value also requires reconciliation with the model prediction. The narrow property ranges and absence of independent batch replication preclude claims of engineering benefit or statistical significance. The original Figure 1 labels the carbon material graphene oxide, whereas the text states graphene nanoplatelets; its chemical identity needs verification. Relative to existing graphene-only, fly-ash-only and other-hybrid studies, the contribution is a material-specific, dual-response process screening rather than demonstrated superiority or a new optimization method.

1. Introduction

Aluminum matrix composites (AMCs) have been widely investigated for aerospace, automotive, and lightweight structural applications because of their low density, high specific strength, and corrosion resistance [1]. Graphene nanoplatelets can enhance hardness and load transfer [2], whereas fly ash offers a low-cost, low-density reinforcement material and provides an opportunity to utilize an abundant by-product of coal combustion [3]. However, achieving these benefits depends on appropriate material processing and reinforcement distribution. The final properties are strongly influenced by reinforcement dispersion, powder deformation during milling, compact integrity, pore evolution, and interfacial reactions during sintering. Consequently, process optimization is necessary

* *Corresponding author.*
E-mail address: irsyadiyani@ft.unsri.ac.id

https://doi.org/10.37934/sej.16.1.234249

to identify parameter combinations that improve hardness without significantly compromising densification.

Graphene nanoplatelets (GNPs) possess high intrinsic strength, elastic modulus, and thermal conductivity and have therefore been used to enhance the mechanical and thermal performance of AMCs [4]. Powder metallurgy studies have demonstrated that small additions of GNPs can significantly increase hardness. For example, an aluminum composite containing 0.1 wt% GNPs exhibited a hardness of approximately 57 HV, nearly 90% higher than that of unreinforced aluminum [6]. Nevertheless, graphene is difficult to disperse uniformly because of strong van der Waals attraction. Excessive graphene content or unsuitable milling conditions can promote agglomeration, localized porosity, and structural damage to graphene. At elevated temperatures, graphene may also react with aluminum to form Al_4C_3. Thus, reinforcement content and processing conditions determine whether graphene facilitates effective load transfer or acts as a source of defects [5, 7].

Fly ash is a heterogeneous particulate by-product that commonly contains silica-, alumina-, and iron-bearing phases. Its low cost, widespread availability, and relatively low density compared with aluminum make it an attractive microscale reinforcement [3, 8]. With adequate particle dispersion and interfacial bonding, fly ash can improve hardness and wear resistance while reducing composite density [9]. A hybrid reinforcement strategy combining graphene at the nanoscale with fly ash at the microscale may therefore provide a balance between material performance, cost, and resource circularity. The primary processing challenge is to achieve uniform dispersion of both reinforcements while minimizing agglomeration and residual porosity.

In powder metallurgy, milling time influences particle refinement, cold welding, fracture, work hardening, and reinforcement redistribution [10, 11]. These competing mechanisms may produce a non-monotonic response, as insufficient milling can result in poor reinforcement dispersion, whereas excessive milling may promote oxidation, particle clustering, and contamination. Sintering temperature and holding time govern interparticle diffusion, neck growth, pore closure, grain evolution, and interfacial reactions [12]. Higher sintering temperatures or longer holding times can improve densification but may also accelerate undesirable interfacial reactions or grain coarsening. Therefore, the four selected processing factors represent distinct but interconnected stages of microstructural development.

Although graphene- and fly-ash-reinforced aluminum composites have been investigated separately, the available literature provides limited directly comparable evidence regarding the combined effects of these reinforcements under the present Taguchi L9 experimental design. This study contributes a nine-condition, dual-response screening of aluminum composites containing combined graphene and fly ash reinforcements (1/4, 2/8, and 3/12 wt%) to evaluate the effects of processing parameters on hardness and bulk density. Unlike studies focusing on individual reinforcements or wear performance, the present investigation compares the relative influence of processing factors on hardness and density within the same experimental design. These findings provide material- and process-specific screening results rather than definitive evidence of a new strengthening mechanism or an optimized process suitable for industrial application. The absence of independent fabrication replicates, interaction-effect estimates, and verification of the carbon reinforcement identity limits the interpretation and generalizability of the findings.

Previous studies have addressed different aspects of the processing challenges associated with aluminum matrix composites. Investigations of graphene-reinforced aluminum composites [2, 5–7] have examined the effects of carbon reinforcement and dispersion but do not directly establish the behavior of aluminum composites containing both graphene and fly ash. Previous optimization studies on fly-ash-reinforced aluminum composites fabricated through powder metallurgy [16] employed a similar processing approach but did not incorporate graphene. Other Taguchi-based

investigations of fly ash hybrid composites [15, 17] considered different secondary reinforcements or focused primarily on wear performance. A previous study on Al/$Y_2W_3O_{12}$/AlN composites [10] investigated milling and sintering parameters in a different hybrid system, while studies on particulate aluminum composites [21–23] provide insights into non-monotonic milling behavior rather than direct validation of the present composite composition. Recent comprehensive reviews [4, 14] provide relevant background information but do not constitute independent experimental benchmarks for the specific aluminum/graphene/fly-ash system investigated in this study. Consequently, these references do not independently establish the superiority of the present composite over a directly comparable hybrid material. The available references also do not provide an independently replicated comparison involving an identical composite composition and processing conditions. Therefore, the research gap is defined by the limited availability of directly comparable factorial studies rather than the absence of previous research on graphene/fly-ash composites.

Comparisons of absolute hardness values across these studies depend on several factors, including aluminum alloy grade, reinforcement chemistry and morphology, processing conditions, porosity, and indentation test load and dwell time. These parameters are not consistently matched across the available studies. Therefore, comparisons with previous investigations primarily highlight the importance of evaluating the trade-offs between reinforcement dispersion and sintering conditions rather than establishing quantitative superiority over previously reported composites.

2. Materials and Experimental Design

2.1 Materials and Fabrication

An aluminum alloy was used as the matrix material, while the carbon reinforcement was supplied by CV Idiora and the fly ash was obtained from the coal-fired power plant of PT Pusri Palembang. The original manuscript identifies the carbon powder as graphene or graphene nanoplatelets (GNPs), whereas Figure 1 identifies the material as graphene oxide (GO). These terms refer to chemically distinct materials. However, information regarding the supplier grade, oxidation state, layer morphology, and supporting characterization data, such as Raman spectroscopy or X-ray photoelectron spectroscopy (XPS), was not provided. Therefore, the identity of the carbon reinforcement remains uncertain and should be verified using the supplier's material certificate or appropriate characterization techniques before manuscript submission. The original material descriptions are provisionally retained. However, conclusions regarding the effects of GNPs or GO should remain tentative until the reinforcement material has been verified.

Three composite compositions were prepared with aluminum/carbon/fly ash weight fractions of 95/1/4, 90/2/8, and 85/3/12 wt%, corresponding to total reinforcement contents of 5, 10, and 15 wt%, respectively. The carbon and fly ash powders were initially heated at 200 °C for 1 h and sieved using the reported 100–400 mesh range. The powders were then weighed, wetted with a 10% ethanol solution for 10 min, and shear-mixed at 300 rpm for 60 min. Subsequently, the mixtures were filtered, dried, and ball-milled for 2, 4, or 6 h. The blended powders were then compacted and sintered according to the prescribed experimental conditions. Figure 1 has been retained for reference; however, its designation of the reinforcement as graphene oxide does not independently confirm that GO was used in the experiments.

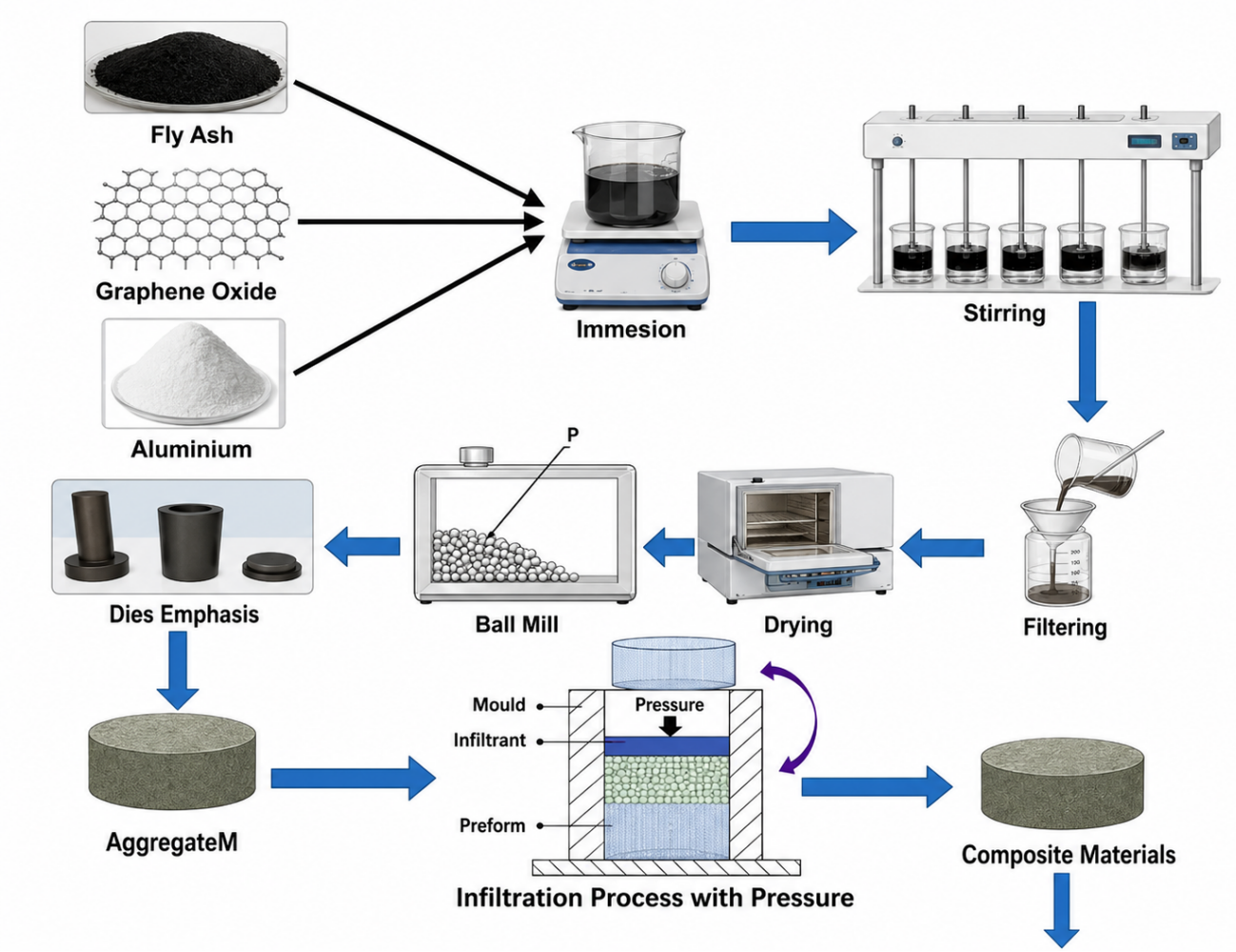


Fig. 1. Fabrication workflow of the aluminum/carbon-reinforcement/fly-ash composite

2.2 Orthogonal Array Design

Four controllable processing factors, each evaluated at three levels, were investigated using a Taguchi L9 (3^4) orthogonal array. The selected factors and their corresponding levels are presented in Table I, while the experimental combinations are summarized in Table II. Vickers hardness was measured in accordance with ISO 6507 and ASTM E384. Three hardness indentations were performed for each experimental condition, and the arithmetic mean was used for subsequent optimization. Bulk density was determined using the Archimedes method. As higher values of both hardness and bulk density were considered desirable, the larger-the-better signal-to-noise (S/N) ratio was employed for both responses. The effects of individual processing factors were evaluated using response means at each factor level, delta values, factor rankings, and percentage contributions derived from the analysis of variance (ANOVA). However, the Taguchi L9 orthogonal array is saturated when four three-level factors are included, leaving no independent residual degrees of freedom for estimating experimental error. Consequently, the ANOVA percentage contributions were interpreted descriptively to assess the relative influence of the processing factors rather than as evidence of statistical significance based on formal F-tests.

Table 1
Processing Factors and Their Corresponding Levels in the Taguchi L9 Orthogonal Array

Factor	Code	Level 1	Level 2	Level 3
Graphene/fly ash fraction	A	5%	10%	15%
Milling time	B	2 h	4 h	6 h
Sintering temperature	C	500 °C	550 °C	600 °C
Holding time	D	0.5 h	1 h	1.5 h

Table 2
Experimental Design Based on the Taguchi L9 (3^4) Orthogonal Array

Run	A: Fraction (%)	B: Milling (h)	C: Sintering (^{0}C)	D: Holding (h)
1	5%	2	500	0.5
2	5%	4	550	1.0
3	5%	6	600	1.5
4	10%	2	550	1.5
5	10%	4	600	0.5
6	10%	6	500	1.0
7	15%	2	600	1.0
8	15%	4	500	1.5
9	15%	6	550	0.5

3. Results and Discussion

The nine experimental conditions employed in the powder metallurgy process were evaluated based on Vickers hardness and bulk density measured using the Archimedes method (Tables 2 and 3). The larger-the-better signal-to-noise (S/N) ratios were analyzed using the Taguchi method to identify and rank the relative influence of the processing factors, while the percentage contributions derived from the sums of squares were interpreted descriptively. As the four three-level factors account for all eight degrees of freedom available in the Taguchi L9 orthogonal array, independent estimation of residual variance and factor interaction effects was not possible. Three hardness indentations were performed for each experimental condition to evaluate within-specimen measurement variability; however, these measurements do not represent independent fabrication replicates or account for between-batch manufacturing variability. The present investigation focused exclusively on the hardness and bulk density of the fabricated composites and did not include face-milling experiments, surface roughness classification, k-nearest neighbors (KNN) modeling, or voting-ensemble methods.

3.1 Hardness and Density

Table 3 presents the Vickers hardness and bulk density results obtained from the nine experimental runs. The mean hardness ranged from 48.13 VHN in Run 5 to 50.07 VHN in Run 9, representing an overall variation of 1.94 VHN across the investigated processing conditions. Meanwhile, the measured bulk density ranged from 2.493 to 2.560 g/cm³, corresponding to an absolute difference of 0.067 g/cm³. The three hardness measurements obtained for each experimental condition demonstrated relatively low variability, with standard deviations ranging from 0.10 to 0.52 VHN and coefficients of variation ranging from 0.20% to 1.06%. These results indicate good repeatability of the hardness indentation measurements within individual specimens. Nevertheless, the relatively low measurement variability does not establish the reproducibility of the

fabrication process, as independent manufacturing replicates were not included in the experimental design.

Table 3
Vickers Hardness and Bulk Density of Aluminum Matrix Composites under Different Experimental Conditions

Run	A	B	C	D	H_1	H_2	H_3	H (VHN)	P (g/cm^3)
1	5	2	500	0.5	49.10	49.90	49.50	49.50	2.497
2	5	4	550	1.0	48.54	49.10	48.90	48.85	2.497
3	5	6	600	1.5	49.30	49.10	49.20	49.20	2.553
4	10	2	550	1.5	49.30	49.50	49.60	49.47	2.547
5	10	4	600	0.5	47.90	48.10	48.40	48.13	2.550
6	10	6	500	1.0	48.80	48.30	49.20	48.77	2.553
7	15	2	600	1.0	50.10	49.90	49.90	49.97	2.543
8	15	4	500	1.5	49.10	48.20	49.10	48.80	2.560
9	15	6	550	0.5	50.20	50.10	49.90	50.07	2.493

3.2 Signal-to-Noise Ratio Analysis

As both hardness and bulk density were considered larger-the-better responses, the signal-to-noise (S/N) ratios were calculated for each experimental run and subsequently averaged at each factor level. Tables IV and V present the mean S/N ratios, delta values, and corresponding factor rankings for hardness and bulk density, respectively. Figures 2 and 3 illustrate the main effects of the investigated processing parameters on the S/N ratios for hardness and bulk density, respectively.

For hardness, milling time (factor B) exhibited the largest S/N delta value of 0.187 dB, indicating the greatest variation in the mean S/N ratio across its investigated levels. This was followed by reinforcement fraction (factor A, 0.145 dB), sintering temperature (factor C, 0.077 dB), and holding time (factor D, 0.013 dB). In contrast, bulk density exhibited a different ranking of processing factors. Holding time (factor D) produced the largest S/N delta value of 0.138 dB, followed closely by sintering temperature (factor C, 0.127 dB) and reinforcement fraction (factor A, 0.119 dB). Milling time (factor B) exhibited the smallest delta value of 0.023 dB, indicating a comparatively limited influence on the bulk density response within the investigated parameter ranges.

These findings indicate that hardness and bulk density exhibit different sensitivities to the investigated processing parameters. Milling time was the dominant factor in the descriptive S/N ranking for hardness, whereas holding time showed the greatest influence on bulk density. This difference suggests that optimizing hardness and bulk density may require different combinations of processing parameters. However, these rankings should be interpreted as descriptive measures of relative factor influence rather than evidence of statistical significance, given the absence of an independent residual error estimate in the saturated Taguchi L9 experimental design.

Table 4
Response of the Signal-to-Noise (S/N) Ratios for Vickers Hardness Using the Larger-the-Better Criterion

Level	A	B	C	D
Level 1	33.836	33.917	33.807	33.844
Level 2	33.766	33.731	33.884	33.837
Level 3	33.911	33.864	33.821	33.831
Delta	0.145	0.187	0.077	0.013
Rank	2	1	3	4

Table 5
Response of the Signal-to-Noise (S/N) Ratios for Bulk Density Using the Larger-the-Better Criterion

Level	A	B	C	D
Level 1	8.012	8.058	8.085	8.004
Level 2	8.131	8.081	8.000	8.066
Level 3	8.069	8.072	8.127	8.142
Delta	0.119	0.023	0.127	0.138
Rank	3	4	2	1

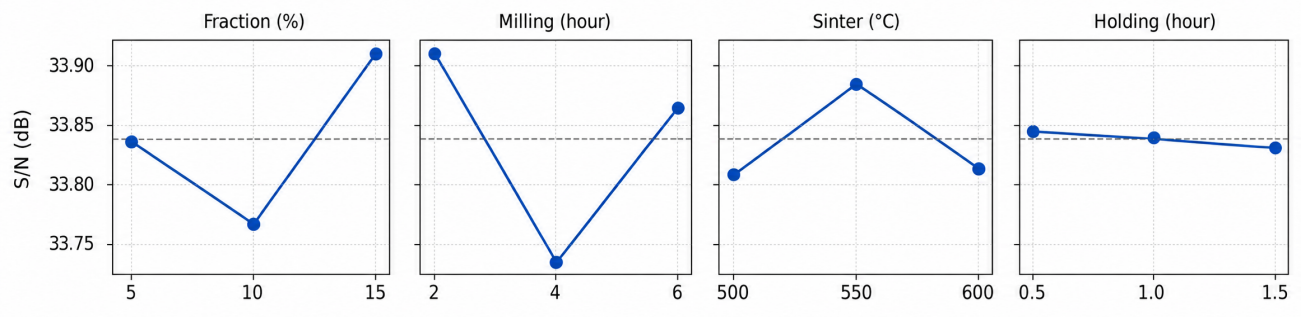


Fig. 2. Main Effects of Processing Parameters on the Signal-to-Noise (S/N) Ratio for Vickers Hardness

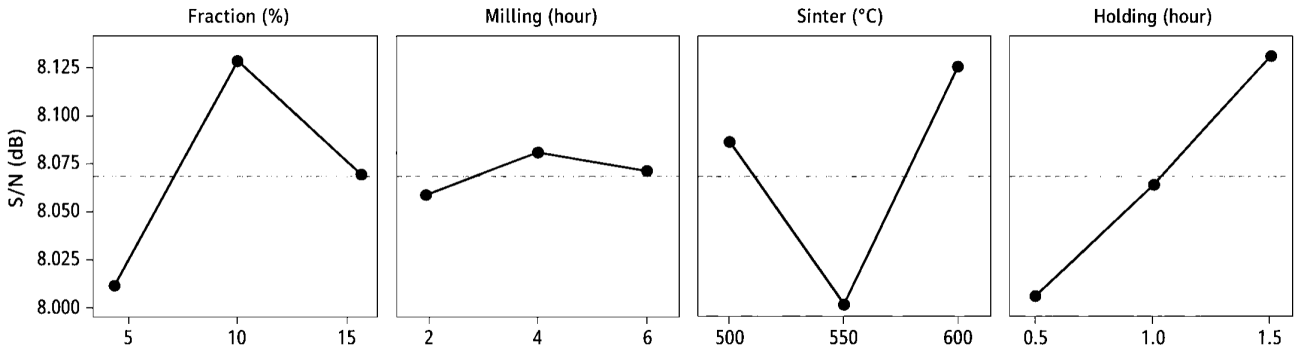


Fig. 3. Main Effects of Processing Parameters on the Signal-to-Noise (S/N) Ratio for Bulk Density

3.3 Analysis of Variance (ANOVA)

Table 6 presents the analysis of variance (ANOVA) results, including the sums of squares and percentage contributions of the investigated processing factors. Figures 4(a) and 4(b) illustrate the percentage contributions of these factors to the observed variations in Vickers hardness and bulk density, respectively.

For hardness, milling time exhibited the highest percentage contribution (56.55%), followed by reinforcement fraction (32.56%), sintering temperature (10.61%), and holding time (0.28%). In contrast, holding time accounted for the largest proportion of the observed variation in bulk density (38.24%), followed by sintering temperature (32.62%), reinforcement fraction (28.07%), and milling time (1.07%). These results indicate that milling time was the predominant factor associated with hardness variation, whereas holding time and sintering temperature were the principal factors associated with bulk density variation within the investigated experimental conditions.

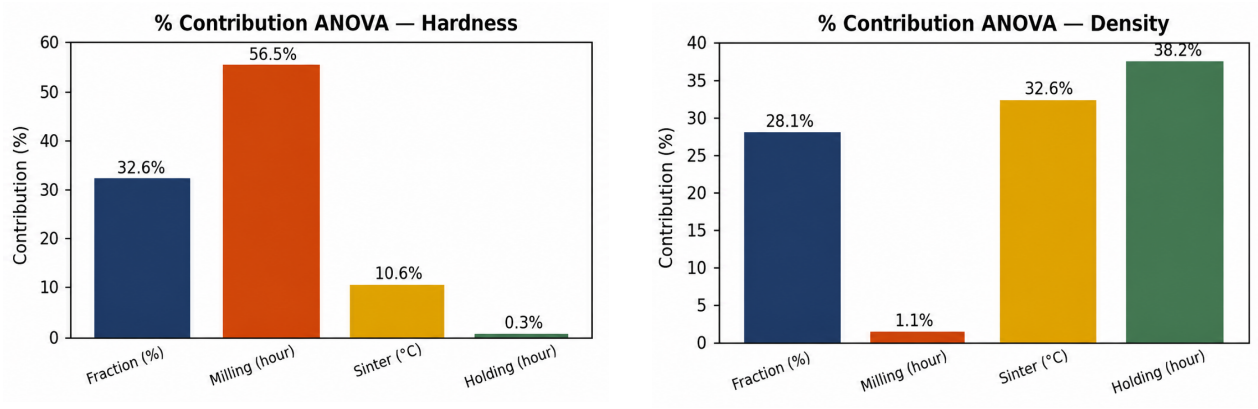
The observed factor rankings are consistent with the expected roles of the processing parameters in powder metallurgy. Milling can influence particle size refinement, powder deformation, and reinforcement dispersion, which may subsequently affect the hardness of the fabricated composites. Conversely, sintering temperature and holding time can influence diffusion, interparticle neck

growth, and pore reduction, thereby affecting the densification behavior and resulting bulk density. However, these mechanisms remain plausible interpretations rather than experimentally confirmed explanations.

It should be emphasized that the four three-level factors in the Taguchi L9 orthogonal array account for all eight available degrees of freedom, leaving no independent residual degrees of freedom for estimating experimental error. Consequently, the percentage contributions reported in Table 6 should be interpreted as descriptive indicators of relative factor influence rather than statistically significant effects. Additional independent fabrication replicates or an appropriately justified pooling of negligible factors would be necessary to estimate residual error and conduct formal statistical significance tests using F- and p-values.

Table 6
Analysis of Variance (ANOVA) and Percentage Contributions of Processing Factors to Vickers Hardness and Bulk Density

Factor	SS (Hardness)	% Contrib.	SS (Density)	% Contrib.
A – Fraction	1.0175	32.56	0.001770	28.07
B – Milling	1.7670	56.55	0.000068	1.07
C – Sintering	0.3315	10.61	0.002056	32.62
D – Holding	0.0088	0.28	0.002411	38.24
Total	3.1248	100.00	0.006305	100.00



(a) (b)

Fig. 4. Percentage contribution of factors from ANOVA for: (a) Hardness, (b) Density

3.4 Statistical Robustness and Practical Effect Size

Across the 27 Vickers hardness indentations obtained from the nine experimental runs, the overall mean hardness was approximately 49.19 VHN. The mean hardness values for individual runs ranged from 48.13 to 50.07 VHN, corresponding to an absolute difference of 1.94 VHN, or approximately 3.9% of the overall mean. The within-run standard deviations ranged from approximately 0.10 to 0.52 VHN, while the coefficients of variation ranged from 0.20% to 1.06%. These relatively low values indicate good repeatability of hardness measurements within the tested specimens. However, they do not provide an estimate of manufacturing variability, as independent fabrication replicates were not included in the experimental design.

Similarly, the measured bulk density ranged from 2.493 to 2.560 g/cm³, representing a relatively small absolute variation of 0.067 g/cm³ across the investigated conditions. Collectively, these findings indicate that the observed differences in hardness and bulk density were relatively limited within the

selected processing parameter ranges. Nevertheless, the measured variations alone are insufficient to establish improvements in load-bearing capacity, wear resistance, service life, or economic performance, as these properties were not directly evaluated. Furthermore, comparisons between the highest and lowest experimental responses should be interpreted cautiously because these values were selected from the same experimental dataset rather than obtained through independent confirmation experiments. Consequently, the observed differences should not be regarded as independently validated processing effects.

3.5 Response Surface Analysis

Figures 5 and 6 illustrate the combined effects of the investigated processing parameters on Vickers hardness and bulk density, respectively. The response surfaces were constructed by interpolating the experimental results obtained from the nine Taguchi L9 design points, with black markers indicating the measured experimental conditions.

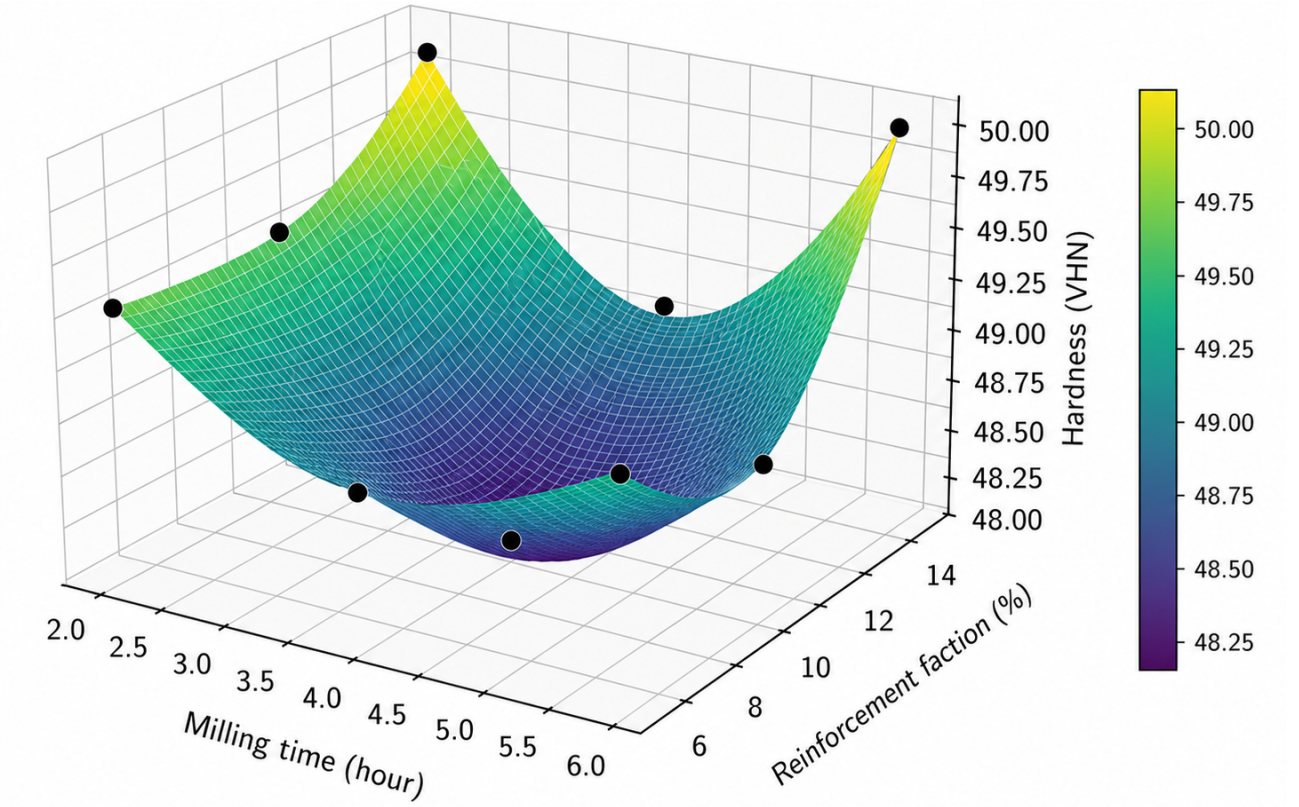


Fig. 5. Response surface of hardness versus milling time and reinforcement fraction

As illustrated in Figure 5, the region associated with higher hardness values corresponds to a higher reinforcement fraction and shorter milling time. This trend may be associated with the contribution of hard reinforcement particles to the composite matrix, provided that the milling process promotes adequate particle distribution. However, prolonged milling may also introduce unfavorable effects, such as particle agglomeration, oxidation, or excessive cold welding, which could influence the resulting hardness. These mechanisms remain possible explanations and require further microstructural characterization for confirmation.

Figure 6 indicates that higher bulk density values are associated with increased sintering temperature and longer holding time. This trend is consistent with the expected enhancement of

diffusion and interparticle bonding during sintering, which may facilitate neck growth and pore reduction. Nevertheless, the observed density differences may also be influenced by variations in reinforcement composition and constituent densities.

As the response surfaces were generated from only nine experimental conditions, and no interaction effects were explicitly assigned or independently estimated in the Taguchi L9 design, the interpolated surfaces should be interpreted primarily as visual representations of the observed trends. They should not be considered independently validated predictive models or used to extrapolate material behavior beyond the investigated processing parameter ranges.

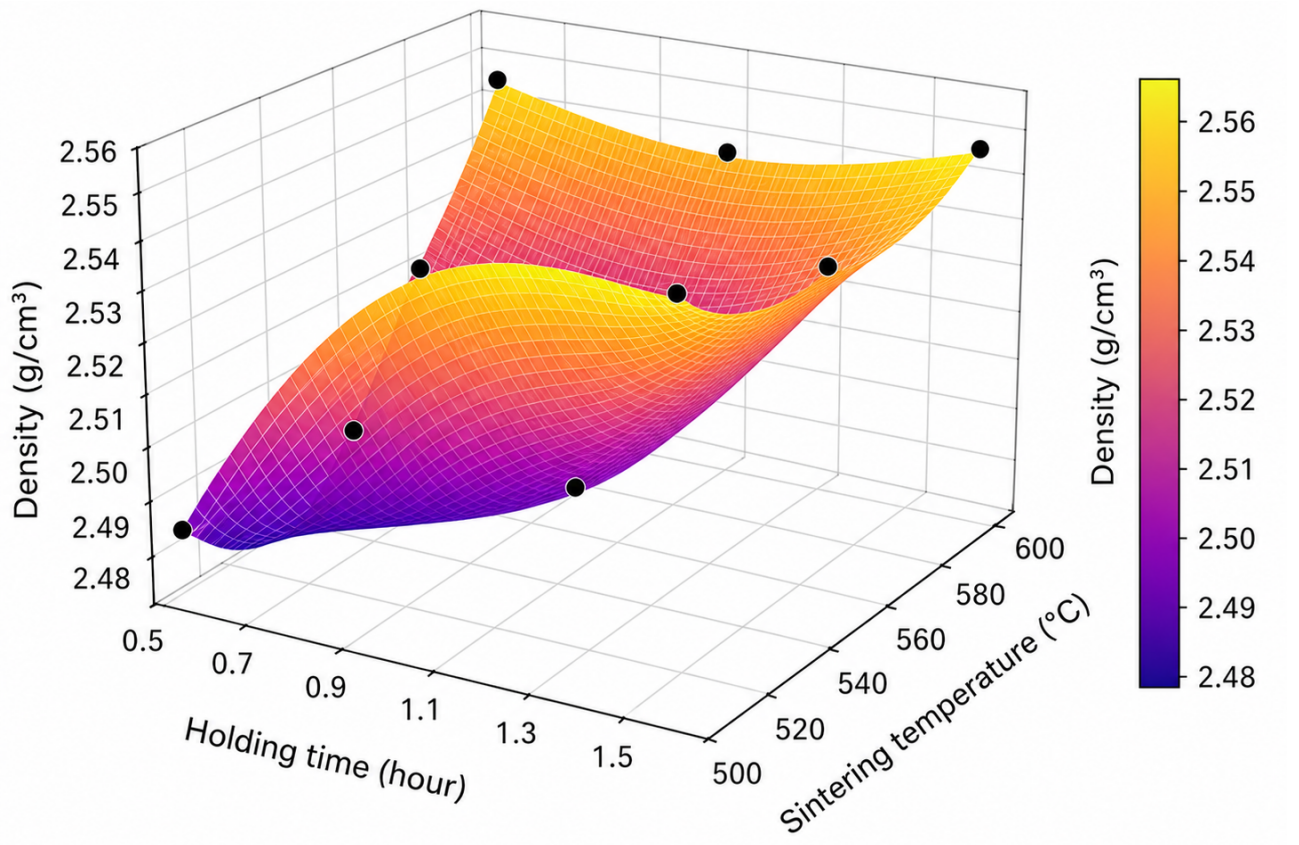


Fig. 6. Response surface of density versus holding time and sintering temperature

3.6 Optimal Processing Conditions and Confirmation Test

Table 7 presents the predicted optimal processing parameter combinations for maximizing Vickers hardness and bulk density based on the Taguchi main-effects analysis. For hardness, the predicted optimal combination was $A_3B_1C_2D_1$, corresponding to a total reinforcement fraction of 15 wt%, milling time of 2 h, sintering temperature of 550 °C, and holding time of 0.5 h. Under these conditions, the predicted Vickers hardness was approximately 50.37 VHN. In contrast, the predicted optimal combination for bulk density was $A_2B_2C_3D_3$, corresponding to a total reinforcement fraction of 10 wt%, milling time of 4 h, sintering temperature of 600 °C, and holding time of 1.5 h. This combination yielded a predicted bulk density of approximately 2.59 g/cm³.

The differences between the predicted optimal combinations indicate that the processing parameters associated with maximum hardness are not identical to those associated with maximum

bulk density. This finding suggests that the two responses exhibit different sensitivities to reinforcement fraction, milling time, sintering temperature, and holding time. Consequently, simultaneous optimization of hardness and bulk density may require a multi-response optimization approach to identify a suitable compromise between the two properties.

The predicted hardness of 50.37 VHN represents an increase of approximately 2.4% relative to the overall experimental mean of 49.19 VHN. A separate confirmation result was reported as showing an approximately 4.4% increase in hardness relative to the same mean, corresponding to an estimated value of 51.35 VHN. However, this reported confirmation result cannot be verified from Table 7, which presents only the predicted responses. The original confirmation measurements and experimental conditions are therefore required to establish whether the reported improvement was obtained experimentally and to explain its difference from the predicted value.

Furthermore, the predicted optimal conditions were determined using an additive main-effects model based on the Taguchi L9 orthogonal array. As independent experimental error and factor interactions could not be estimated from the saturated design, these results should be interpreted as preliminary optimization predictions. Additional independent confirmation experiments are necessary to assess the reproducibility, statistical uncertainty, and practical significance of the predicted improvements.

Table 7
Predicted Optimal Processing Parameter Combinations and Corresponding Vickers Hardness and Bulk Density Values

Response	Optimum combination	Prediction
Hardness	$A_3B_1C_2D_1$ (15%, 2 h, 550 °C, 0.5 h)	≈ 50.37 VHN
Density	$A_2B_2C_3D_3$ (10%, 4 h, 600 °C, 1.5 h)	≈ 2.59 g/cm³

3.7 Comparison with Previous Studies and Research Contributions

The present study recorded Vickers hardness values ranging from 48.13 to 50.07 VHN and bulk density values ranging from 2.493 to 2.560 g/cm³. Comparisons with previous studies should be interpreted cautiously because differences in material composition, reinforcement characteristics, fabrication methods, and testing conditions may influence the reported properties. Previous investigations of graphene-reinforced aluminum composites [2, 5–7] employed different carbon contents, aluminum alloys, and processing techniques, while studies involving fly-ash-reinforced aluminum composites [3, 8, 9, 16, 24] differed in their reinforcement compositions and fabrication routes. Similarly, studies employing Taguchi optimization for hybrid-reinforced composites [10, 15, 17] investigated different material systems or response variables. Although recent reviews [4, 14] provide useful insights into reinforcement behavior and processing trends, they cannot substitute for direct experimental comparisons under equivalent conditions. Consequently, differences in absolute hardness values alone cannot establish superior performance without considering the aluminum matrix, reinforcement characteristics, porosity, and hardness testing procedures. The principal contribution of the present study is therefore the comparative evaluation of processing-factor influences on hardness and bulk density within the investigated experimental design, rather than a demonstrated performance advantage over previously reported composites.

3.7.1 Influence of milling time on hardness

Milling time exhibited the highest percentage contribution to hardness variation (56.55%), which may be associated with the competing mechanisms occurring during mechanical alloying. Repeated particle deformation, fracture, and cold welding can promote particle refinement, increase defect density, and improve reinforcement distribution, potentially enhancing composite hardness [21, 22]. However, prolonged milling may also introduce unfavorable effects, including oxidation, contamination, carbon-reinforcement damage, and particle agglomeration [22, 23]. The present results revealed a non-monotonic response, with the highest mean hardness S/N ratio occurring at 2 h of milling, the lowest at 4 h, and an intermediate value at 6 h. This trend indicates that extending the milling duration did not consistently improve hardness within the investigated range. The shorter milling duration may have provided a more favorable balance between reinforcement distribution and milling-induced microstructural changes. Nevertheless, particle-size analysis and microstructural characterization are necessary to verify the mechanisms responsible for this behavior.

3.7.2 Influence of sintering parameters on bulk density

Holding time and sintering temperature collectively accounted for 70.86% of the observed bulk density variation. This result is consistent with the expected role of thermal processing in powder metallurgy, where increased thermal exposure can promote atomic diffusion, interparticle neck formation, particle bonding, and pore reduction [10, 12]. Previous Taguchi-based investigations of Al–5% fly-ash powder metallurgy composites identified thermal and compaction-related parameters as important factors influencing density and hardness [16]. Similarly, studies involving multi-response optimization of Al–Si/fly-ash composites have reported improvements in material properties associated with sintering conditions [14]. In the present study, the predicted optimal bulk density was associated with a sintering temperature of 600 °C and a holding time of 1.5 h. Although this result is consistent with established sintering mechanisms, further microstructural examination is required to determine whether the observed density variations resulted primarily from pore reduction, phase formation, or differences in constituent composition.

3.7.3 Potential formation of Al_4C_3 and interfacial effects

The maximum sintering temperature of 600 °C raises the possibility of interfacial reactions between the aluminum matrix and carbon reinforcement. Previous investigations have reported that aluminum carbide (Al_4C_3) may form at graphene–aluminum interfaces, with its formation and morphology influenced by processing temperature and thermal exposure [18–20]. Depending on its distribution and morphology, interfacial carbide formation may influence matrix–reinforcement bonding and mechanical behavior. However, excessive or continuous carbide formation may adversely affect interfacial integrity and environmental stability. The relatively modest contribution of sintering temperature to hardness variation (10.61%) could reflect competing effects associated with densification, interfacial bonding, and possible reaction-product formation. Nevertheless, these explanations remain hypothetical because direct phase identification and interfacial characterization using techniques such as X-ray diffraction, Raman spectroscopy, and high-resolution microscopy were not performed.

3.7.4 Influence of reinforcement fraction on hardness and bulk density

Reinforcement fraction ranked second in its contribution to hardness variation and third in its contribution to bulk density variation, indicating that changes in reinforcement content were associated with both measured responses. Increasing reinforcement content may enhance hardness through mechanisms such as load transfer, grain refinement, dislocation strengthening, and the incorporation of hard fly-ash particles. Conversely, higher reinforcement contents may increase the likelihood of particle agglomeration, interfacial void formation, and resistance to powder compaction [5, 7]. In the present investigation, Run 9, containing 15 wt% total reinforcement, exhibited the highest measured hardness but also the lowest bulk density. This observation highlights a potential trade-off between hardness and bulk density within the investigated compositions. However, because reinforcement fraction also changes the theoretical density of the composite, the lower measured bulk density cannot be attributed solely to reduced densification. Additional measurements of relative density and porosity are required to distinguish compositional effects from consolidation behavior.

3.7.5 Research contribution and methodological limitations

The application of the Taguchi method for processing-parameter optimization is well established [13, 15–17]. Therefore, the contribution of the present study lies in evaluating the relative influences of reinforcement fraction, milling time, sintering temperature, and holding time on two material responses within the investigated aluminum/carbon-reinforcement/fly-ash composite system. The descriptive ANOVA results indicated that milling time accounted for the largest proportion of observed hardness variation (56.55%), whereas holding time (38.24%) and sintering temperature (32.62%) were the principal contributors to bulk density variation. These percentages represent the allocation of variation among the fitted main effects and should not be interpreted as statistically significant causal effects.

Several limitations should be acknowledged, including the absence of directly comparable carbon-only and fly-ash-only control specimens, independent fabrication replicates, interaction estimates, and comprehensive microstructural characterization. In addition, the precise identity of the carbon reinforcement requires verification, and the economic implications of the proposed processing conditions were not experimentally evaluated. Future investigations should incorporate matched control materials, independent confirmation experiments, and quantitative analyses of reinforcement distribution, phase composition, and porosity to establish the underlying mechanisms and practical significance of the observed trends.

4. Conclusion

This study investigated the effects of reinforcement fraction, milling time, sintering temperature, and holding time on the Vickers hardness and bulk density of aluminum/carbon-reinforcement/fly-ash composites fabricated using powder metallurgy. A Taguchi L9 orthogonal array was employed to evaluate four processing factors at three levels. The measured hardness ranged from 48.13 to 50.07 VHN, while bulk density varied from 2.493 to 2.560 g/cm^3. Descriptive analysis of variance indicated that milling time exhibited the highest contribution to hardness variation (56.55%), followed by reinforcement fraction (32.56%). In contrast, holding time (38.24%) and sintering temperature (32.62%) were the dominant contributors to bulk density variation. These findings demonstrate that hardness and bulk density exhibit different sensitivities to the investigated processing parameters.

Based on the Taguchi main-effects model, the predicted optimal combination for hardness was 15 wt% total reinforcement, 2 h milling, 550 °C sintering temperature, and 0.5 h holding time, yielding an estimated hardness of 50.37 VHN. The predicted optimal combination for bulk density was 10 wt% total reinforcement, 4 h milling, 600 °C sintering temperature, and 1.5 h holding time, corresponding to an estimated density of 2.59 g/cm³. These different parameter combinations indicate that simultaneous improvement of both responses may require a multi-response optimization approach. Although an approximately 4.4% improvement in hardness was reported from a confirmation test, the absence of the original measurements and independent fabrication variability prevents verification of this result and assessment of its statistical uncertainty.

The principal contribution of this study is the identification and comparative ranking of processing parameters associated with hardness and bulk density variations within the investigated composite system. However, the relatively narrow response ranges, absence of independent fabrication replicates, and saturated Taguchi L9 design limit the statistical interpretation and generalizability of the findings. Furthermore, the identity of the carbon reinforcement must be confirmed to resolve the inconsistent terminology referring to graphene oxide and graphene nanoplatelets. Future investigations should incorporate independently fabricated confirmation specimens, appropriate single-reinforcement and hybrid control materials, and comprehensive microstructural characterization using scanning electron microscopy, energy-dispersive X-ray spectroscopy, Raman spectroscopy, X-ray photoelectron spectroscopy, X-ray diffraction, and porosity measurements. These additional investigations would help establish the reproducibility, underlying strengthening and densification mechanisms, and potential engineering applicability of the developed composites.

Acknowledgement
This work was supported by Universitas Sriwijaya.

Conflict of Interest Statement
The authors declare that there is no conflict of interest regarding the publication of this paper. No financial support, grants, or other forms of compensation were received that could have influenced the outcomes of this work. The research was conducted in the absence of any commercial or financial relationships that could be construed as a potential conflict of interest.

Author Contributions Statement
Qomarul Hadi: Conceptualization, Methodology, Investigation, Data curation, Formal analysis, Visualization, Writing – original draft.
Irsyadi Yani: Conceptualization, Methodology, Validation, Supervision, Writing – review & editing.
Nukman: Methodology, Investigation, Resources, Validation, Writing – review & editing.
Agung Mataram: Methodology, Formal analysis, Validation, Visualization, Writing – review & editing.
All authors have reviewed and approved the final version of the manuscript and agreed to be accountable for their respective contributions to the work.

Data Availability Statement
All data generated or analyzed during this study are included in this published article. Additional datasets are available from the corresponding author upon reasonable request. Where applicable, publicly available datasets used in the study are cited in the references.

Ethics Statement

This study was conducted in accordance with the ethical standards of the institutional and/or national research committee. Ethical approval was obtained where required, and informed consent was obtained from all participants involved in the research.

References

[1] Miracle, D.B. (2005). Metal matrix composites – From science to technological significance. Composites Science and Technology, 65(15–16), 2526–2540.
[2] Rashad, M., Pan, F., Tang, A., & Asif, M. (2015). Effect of graphene nanoplatelets on the mechanical properties of aluminum composites. Materials & Design, 88, 145–153.
[3] Rohatgi, P.K., Guo, R.Q., & Huang, P. (2004). Fly ash-based aluminum composites. Journal of Materials Science, 39, 2969–2977.
[4] Lin, F., Ren, M., Jia, F., & Jiang, Z. (2025). Graphene-reinforced aluminium matrix nanocomposites: Fabrication, properties and applications. Advanced Nanocomposites, 2, 59–85.
[5] Liu, J., et al. (2023). Influence of graphene content on the microstructure and properties of GNPs/Al composites. International Journal of Electrochemical Science, 18(10), 100320.
[6] Tabandeh-Khorshid, M., Omrani, E., Menezes, P.L., & Rohatgi, P.K. (2018). Mechanical and tribological behaviours of aluminium matrix composites reinforced by graphene nanoplatelets. Engineering Science and Technology, an International Journal, 21(4), 623–629.
[7] Rodríguez-González, C., et al. (2023). Effect of nanocarbon on the structural and mechanical properties of 6061 aluminum composites by powder metallurgy. Metals / Nanomaterials (MDPI), 13(11), 674644.
[8] Tiwari, S.K., Rao, A.U., Dasgotra, A., & Kona, S. (2021). Characterization of aluminum-fly ash composite fabricated by stir casting technique. Materials Today: Proceedings, 46, 2179–2182.
[9] Ramachandra, M., & Radhakrishna, K. (2007). Effect of reinforcement of fly ash on sliding wear, slurry erosive wear and corrosive behaviour of aluminium matrix composite. Wear, 262(11–12), 1450–1462.
[10] Sethi, H., Das, S., & Das, K. (2021). Evaluating the influence of milling time, sintering temperature and time on the microstructural changes and mechanical properties of Al-Y2W3O12-AlN hybrid composites. Powder Technology, 377, 244–256.
[11] Fogagnolo, J.B., Ruiz-Navas, E.M., & Simón, M.A. (2003). Powder metallurgy processing of aluminum matrix composites. Materials Science and Engineering A, 355(1–2), 50–55.
[12] German, R.M. (2005). Powder Metallurgy and Particulate Materials Processing. Princeton, NJ: Metal Powder Industries Federation.
[13] Taguchi, G. (1990). Introduction to Quality Engineering. Tokyo: Asian Productivity Organization.
[14] Anwar, S., et al. (2025). Fly ash as a sustainable reinforcement in composite materials: a comprehensive review on enhancing mechanical properties for eco-friendly engineering. Discover Materials, 5, 331.
[15] Vinoth Kumar, S., et al. (2023). Parametric optimization of wear parameters of hybrid composites (LM6/B4C/fly ash) using Taguchi technique. Frontiers in Mechanical Engineering, 9, 1279481.
[16] Arita, Y., & Hayati, R. (2012). Taguchi method approach to optimize manufacturing process parameters of aluminum-5% fly ash alloy using powder metallurgy. Advanced Materials Research, 576, 284–287.
[17] Neelima Devi, C., et al. (2021). Taguchi analysis for sliding wear characteristics of carbon nanotube-fly ash reinforced aluminium nanocomposites. Journal of King Saud University – Engineering Sciences / PMC, 33, 7887386.
[18] Contreras-Cuevas, A., et al. (2026). Effect of aluminum carbide (Al4C3) on the mechanical properties of aluminum matrix composites reinforced with graphene nanoplatelets. Metals (MDPI), 16(4), 408.
[19] Ramírez, C., et al. (2021). Mechanical characterization of graphene–aluminum nanocomposites: In-situ study of Al4C3 formation. Materials Today: Proceedings, 44, 3823–3828.
[20] Nayak, K.C., et al. (2023). Microstructural characteristics of Al4C3 phase and the interfaces in Al/graphene nanoplatelet composites and their effect on the mechanical properties. Journal of Materials Engineering and Performance, 32, 10432–10445.
[21] Alizadeh, A., et al. (2024). Effect of milling time and reinforcement volume fraction on microstructure and mechanical properties of SiCp-reinforced AA2017 composite powder produced by high-energy ball milling. Materials (MDPI), 17(2), 435.
[22] Prakash, K.S., et al. (2017). Effect of milling time on the microstructure, physical and mechanical properties of Al-Al2O3 nanocomposite synthesized by ball milling and powder metallurgy. Materials (MDPI), 10(11), 1232.
[23] Sathish, T., et al. (2023). Effect of blending duration on physical, mechanical and tribological behavior of aluminum matrix composites: An experimental analysis. Materials Today: Proceedings / ScienceDirect, S2214785323047174.

[24] Razzaq, A.M., Abdul Majid, D.L.A., Ishak, M.R., & Uday, M.B. (2017). Microstructural characterization of fly ash particulate reinforced AA6063 aluminium alloy for aerospace applications. IOP Conf. Ser. Mater. Sci. Eng., 270(1), 012028.